Photoacoustic correlation spectroscopy for calibration-free absolute quantification of particle concentration

Yong Zhou, Junjie Yao, Konstantin I. Maslov, Lihong V. Wang

Yong Zhou, Junjie Yao, Konstantin I. Maslov, Lihong V. Wang, "Photoacoustic correlation spectroscopy for calibration-free absolute quantification of particle concentration," Proc. SPIE 8943, Photons Plus Ultrasound: Imaging and Sensing 2014, 89431W (3 March 2014); doi: 10.1117/12.2036635

SPIE.

Event: SPIE BiOS, 2014, San Francisco, California, United States

Photoacoustic correlation spectroscopy for calibration-free absolute quantification of particle concentration

Yong Zhou, Junjie Yao, Konstantin I. Maslov, Lihong V. Wang*
Optical Imaging Laboratory, Department of Biomedical Engineering, Washington University in St. Louis, One Brookings Drive, St. Louis, MO 63130, USA
*Address all correspondence to: LHWANG@WUSTL.EDU

Abstract

Currently, laser fluence calibration is typically required for quantitative measurement of particle concentration in photoacoustic microscopy. In this paper, we present another quantitative approach to measure absolute absorber concentrations by photoacoustic correlation spectroscopy. The proposed method is based on the fact that the Brownian motion induces particle count fluctuation in the detection volume. We first derived a theoretical model for photoacoustic signals and then applied our method to quantitative measurement of different concentrations of various particles. The experimental results agreed well with the predictions from the theoretical model, suggesting that our method can be used for absolute particle concentrations measurement.
Keywords: photoacoustic imaging, Poisson distribution, particle concentration, calibration free, red blood cell

1. Introduction

Over the past few years, photoacoustic microscopy (PAM) has been proven to be capable of structural, functional, molecular, and metabolic imaging.[1-9] In PAM, the object is illuminated by a short-pulsed laser beam. Following the absorption of light, the increased temperature generates an initial pressure rise, which propagates as photoacoustic (PA) waves and is detected by an ultrasonic transducer. Because the initial pressure is directly proportional to the absorbed optical energy density $A(\vec{r})$ ($\mathrm{J\cdot m^{-3}}$) in the tissue, which is the product of the optical fluence $F(\vec{r})$ ($\mathrm{J\cdot m^{-2}}$) and the optical absorption coefficient $\mu_a(\vec{r})$ ($\mathrm{m^{-1}}$), multi-wavelength PA measurements can provide spectral information of optical absorption. So far, PAM has shown its viability in detecting many intrinsic contrasts in biological tissues, such as hemoglobin, bilirubin, DNA and RNA in nuclei, lipid, cytochromes, and melanin. To obtain the intrinsic contrast property $\mu_a(\vec{r})$, we need to compensate for the extrinsic quantity $F(\vec{r})$. However, the optical fluence is usually unknown because of the light attenuation in tissue. Therefore, it is generally challenging to provide quantitative PA studies of, for example, oxygen metabolism.

In this paper, we present a quantitative approach to measure absolute absorber concentrations by statistical analyses of PA signals. To obtain a fluence-independent detection, the particle count in the detection volume needs to be small enough so that PA signal fluctuation due to the particle Brownian motion is dominant compared to other fluctuating sources, such as laser intensity fluctuation, electronic thermal noise, and photon shot noise. The paper is organized as follows. We first developed a model to describe the relationship between the measured PA signals and the particle counts. The principle was then demonstrated experimentally by using microsphere with varied concentrations.

2. Methods and Materials

Particle fluctuation in a detection volume caused by Brownian motion is governed by Poisson distribution. Thus, the variance of the particle count (N_p) equals its mean, i.e.,

$$Var(N_p) = E(N_p). \quad (1)$$

Fluctuations of the particle count contribute to the PA signal fluctuations, which were assessed with multiple laser pulses. However, other sources could also lead to fluctuations in the PA signal, such as laser intensity fluctuation, electronic thermal noise, and photon shot noise. Because the photon shot noise is much smaller than the electronic thermal noise in PAM, it can be ignored. In a typical PA system, a photodiode (PD) is used to compensate for the

Photons Plus Ultrasound: Imaging and Sensing 2014, edited by Alexander A. Oraevsky, Lihong V. Wang,
Proc. of SPIE Vol. 8943, 89431W · © 2014 SPIE · CCC code: 1605-7422/14/$18 · doi: 10.1117/12.2036635

laser pulse energy fluctuations. A beam sampler is used to extract a small portion of light into PD, while the remaining light illuminates the sample. The output of photodiode amplitude (A_{PD}) can be expressed as

$$A_{PD} = k_{PD} R N_{ph} + n_{PD}, \tag{2}$$

where k_{PD} is the efficiency of conversation from photons to voltage; R is the percentage that light reflects from the beam sampler; N_{ph} is the photon count of the incident light; and n_{PD} is the PD electronic thermal noise. The photon count fluctuation is typically specified as a few percent of average pulse energy, hence the variance of photon count fluctuation can be assumed to be proportional to the square of mean photon counts:

$$Var(N_{ph}) = \alpha^2 E^2(N_{ph}), \tag{3}$$

where Var() denotes variance, E() denotes mean, and α denotes the photon count fluctuation coefficient. Parameter α is a property of the laser but it can be controlled to some extent by discarding laser pulses outside of the predetermined range of pulse energies.

Because the thermal noise is zero-mean, the mean and variance of A_{PD} are derived from Eq. (2) as

$$E(A_{PD}) = k_{PD} R E(N_{ph}), \tag{4}$$

$$Var(A_{PD}) = k_{PD}^2 R^2 Var(N_{ph}) + Var(n_{PD}). \tag{5}$$

Based on Eqs. (4) and (5), we have

$$Var(A_{PD}) = \alpha^2 E^2(A_{PD}) + Var(n_{PD}). \tag{6}$$

Eq. (6) shows a parabolic relationship between $Var(A_{PD})$ and $E(A_{PD})$.

Similar to the analysis of PD, the PA amplitude (A_{PA}) can be expressed as

$$A_{PA} = k_{PA} N_p T N_{ph} + n_{PA}, \tag{7}$$

where k_{PA} is a constant factor including Grueneisen parameter, heat conversion percentage, absorption cross section, and other minor contributors; N_p is the particle count inside the detection volume; T is the percentage that light transmits through the beam sampler; and n_{PA} is the electronic thermal noise of the ultrasonic transducer. Note that R + T is slightly less than unity due to absorption and scattering loss.

Based on Eq. (7), the mean and the variance of A_{PA} are

$$E(A_{PA}) = k_{PA} E(N_p) T E(N_{ph}), \tag{8}$$

$$\begin{aligned} Var(A_{PA}) &= k_{PA}^2 Var(N_p T N_{ph}) + Var(n_{PA}) \\ &= k_{PA}^2 T^2 [Var(N_p) E^2(N_{ph}) + Var(N_{ph}) E^2(N_p) + Var(N_p) Var(N_{ph})] + Var(n_{PA}) \end{aligned}. \tag{9}$$

Substituting Eq. (1) into Eq. (9), we have

$$\begin{aligned} Var(A_{PA}) &= k_{PA}^2 T^2 [E(N_p) E^2(N_{ph}) + Var(N_{ph}) E^2(N_p) + E(N_p) Var(N_{ph})] + Var(n_{PA}) \\ &= k_{PA}^2 T^2 [E(N_p) E^2(N_{ph}) + (E^2(N_p) + E(N_p)) \alpha^2 E^2(N_{ph})] + Var(n_{PA}) \end{aligned}. \tag{10}$$

When $E(N_p) \gg \alpha^{-2}$, we have

$$\begin{aligned} Var(A_{PA}) &\approx k_{PA}^2 E^2(N_p) \alpha^2 T^2 E^2(N_{ph}) + Var(n_{PA}) \\ &= \alpha^2 E^2(A_{PA}) + Var(n_{PA}) \end{aligned}. \tag{11}$$

The ratio between the mean squared and the variance of A_{PA} is the power-based signal-to-noise ratio (SNR):

$$SNR_{PA} = \frac{E^2(A_{PA})}{Var(A_{PA})} = \frac{(k_{PA}E(N_p)TE(N_{ph}))^2}{k_{PA}^2T^2[E(N_p)E^2(N_{ph}) + (E^2(N_p) + E(N_p))\alpha^2E^2(N_{ph})] + Var(n_{PA})} \quad (12)$$

Defining $SNR_{th} = \frac{E^2(A_{PA})}{Var(n_{PA})}$, and substituting it into Eq. (12), we have

$$\frac{1}{SNR_{PA}} = \frac{1}{E(N_p)} + (1 + \frac{1}{E(N_p)})\alpha^2 + \frac{1}{SNR_{th}} = (1+\alpha^2)\frac{1}{E(N_p)} + \frac{1}{SNR_{th}} + \alpha^2 . \quad (13)$$

Since $\alpha^2 \ll 1$, we get

$$\frac{1}{SNR_{PA}} \approx \frac{1}{E(N_p)} + \frac{1}{SNR_{th}} + \alpha^2 . \quad (14)$$

Eq. (14) can be discussed in two different cases. In case 1, when particles are dense enough so that $E(N_p) \gg \alpha^{-2}$, we have

$$\frac{1}{SNR_{PA}} \approx \frac{1}{SNR_{th}} + \alpha^2 . \quad (15)$$

SNR_{PA} approaches α^{-2} when SNR_{th} increases. In case 2, when particles are sparse enough so that $E(N_p) \ll \alpha^{-2}$, we have

$$\frac{1}{SNR_{PA}} \approx \frac{1}{E(N_p)} + \frac{1}{SNR_{th}} . \quad (16)$$

SNR_{PA} approaches $E(N_p)$ when SNR_{th} increases. Using Eq. (16) or more generally Eq. (14), one can measure the expected value of the absolute particle count. In addition, if $E(N_p) \ll SNR_{th}$, Eq. (16) reduces to

$$SNR_{PA} \approx E(N_p) . \quad (17)$$

Thus, the measurement outcome is independent of the laser fluence. Although our model is derived for static particle suspension, it is also valid for flowing particles, because the temporal statistics of particle count fluctuations in a static medium are equivalent to the spatial statistics of the particle count fluctuations in a flowing medium.[24]

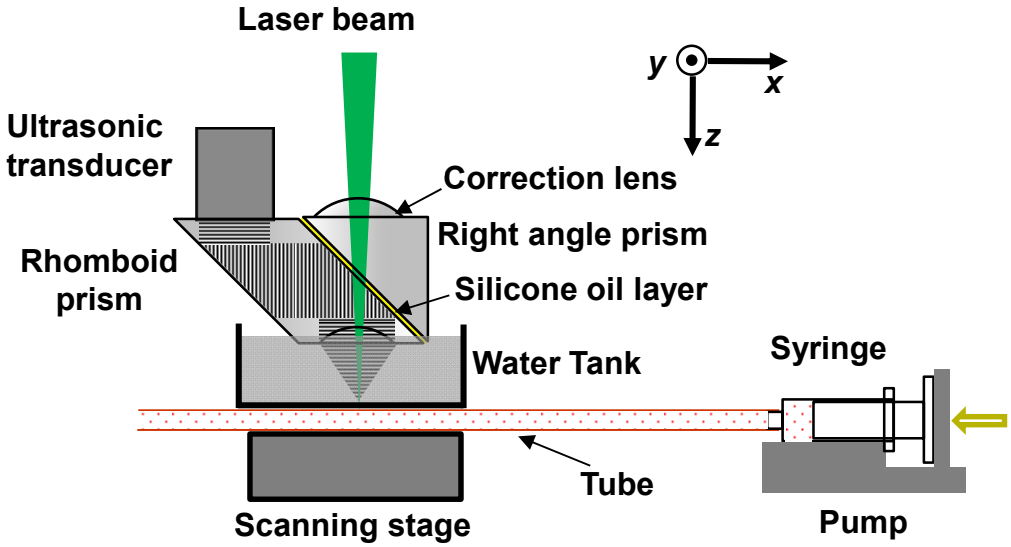

Fig. 1 System schematic used in the experiment.

We validated this idea using our optical-resolution PAM (OR-PAM) system shown in Fig. 1. So far, this OR-PAM system has achieved a lateral resolution of ~5 μm and an axial resolution of ~15 μm with an imaging depth of ~1 mm. Thus, the detection volume is about 500 μm^3 based on 1/e excitation beam width. In all experiments, plastic tubing with inner diameter of 300 μm was used to flow the liquid sample. A fast flow speed of 9 mm/s was applied to the fluid in the tubing to avoid potential heat aggregation or photobleaching, and to make sure the multiple PA signals were completely independent.

Lysed bovine blood was used for the experiment with large particle counts. It is estimated that there are about one billion hemoglobin molecules in the detection volume, which satisfies the condition that $E(N_p)$ is much larger than α^{-2} for Eq. (15). For small particle counts, defibrinated whole bovine blood was used instead for the experiment. In whole blood, RBCs, instead of hemoglobin molecules, constitute the particles moving in and out of the detection volume. Since there are only a few RBCs in the detection volume, $E(N_p)$ will be much smaller than α^{-2}, satisfying the condition for Eq. (16).

To demonstrate quantitative particle count measurement, we prepared samples with different particle concentrations. Since we require that particle count fluctuation is dominant in the PA signal fluctuation, two different sizes of red dyed microspheres were used to make the samples: the 0.5 μm diameter particle with a stock concentration of ~3.64×10^{11} particles per milliliter (2.5% w/w), and the 1 μm diameter particle with a stock concentration of ~4.55×10^{10} particles per milliliter (2.5% w/w). The small-sized particle stock solution was diluted by 2 and 4 times, while the large-sized particle stock solution was diluted to 8 and 16 times the stock concentration of the small-sized particle solution.

3. Results

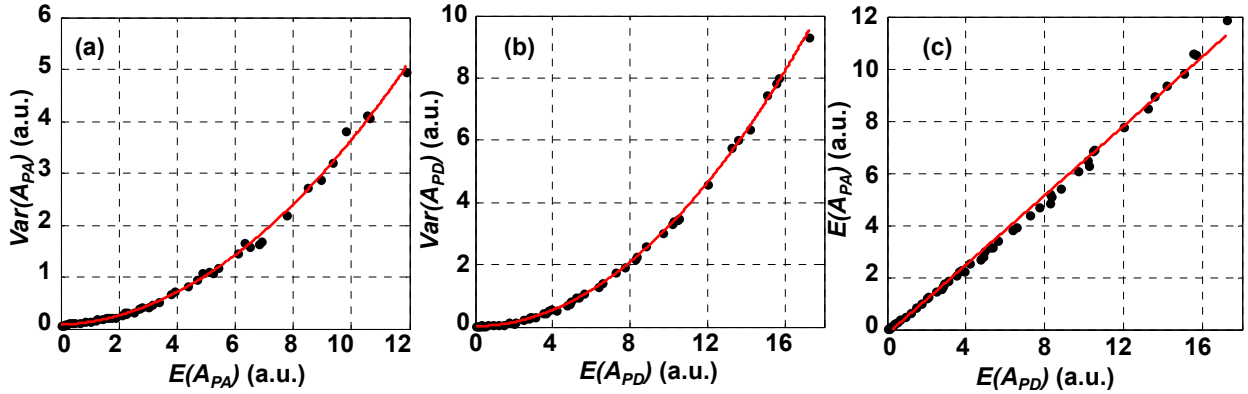

Fig. 2 Relationship between Var(A_{PA}) and E(A_{PA}) (a), Var(A_{PD}) and E(A_{PD}) (b), E(A_{PA}) and E(A_{PD}) (c). Black dots: experimental data. Red lines: theoretical fitting. (a) fitting equation: $Y= \alpha^2x^2+7508$, where α=0.0576. (b) fitting equation: $Y=\beta^2x^2+2631$, where β=0.0567. (c) fitting equation: Y=0.6656x-190.7.It shows that when particle number is extremely large, both Var(A_{PA}) and Var(A_{PD}) follow parabolic relationship with respect to E(A_{PA}) and E(A_{PD}), respectively. The coefficient α and β are almost identical, both from light fluctuation. (c) shows there is a good linearity between E(A_{PA}) and E(A_{PD}).

Based on Eqs. (6) and (11), $Var(A_{PD})$ and $Var(A_{PA})$ parabolically depend on $E(A_{PD})$ and $E(A_{PA})$, respectively. In addition, $E(A_{PA})$ should be proportional to $E(A_{PD})$. In the experiment using lysed bovine blood, the result shows a clear parabolic relationship between $Var(A_{PA})$ and $E(A_{PA})$ [Figure 2(a)]. The photon count fluctuation coefficient α was fitted to be 5.67%, close to the laser specification. The similar result between $Var(A_{PD})$ and $E(A_{PD})$ is shown in Fig. 2(b). The coefficient α was fitted to be 5.76%, very close to the one for PD. In addition, Fig. 2(c) shows that there is a good linearity between $E(A_{PA})$ and $E(A_{PD})$.

As mentioned above, we can regroup the laser pulses based on the photodiode readings. By doing this, the laser intensity fluctuation coefficient α can be artificially controlled to a predetermined value. Fig. 3(a) shows that with large particle counts, SNR_{PA} is dominated by the light fluctuations when SNR_{th} increases, consistent with Eq. (15).

Here the neutral density filter was adjusted to change the laser fluence and thus to change the SNR_{th}. On the other hand, when the particle counts are small in the detection volume, the measurement results with high SNR_{th} only rely on the particle counts [Figs. 3(b) to (d)], consistent with Eq. (16). Although the photon count fluctuation coefficients are varied, the measurement results stay the same. Thus, the fluence-independent measurement is achieved with the conditions of high SNR_{th} and small particle counts.

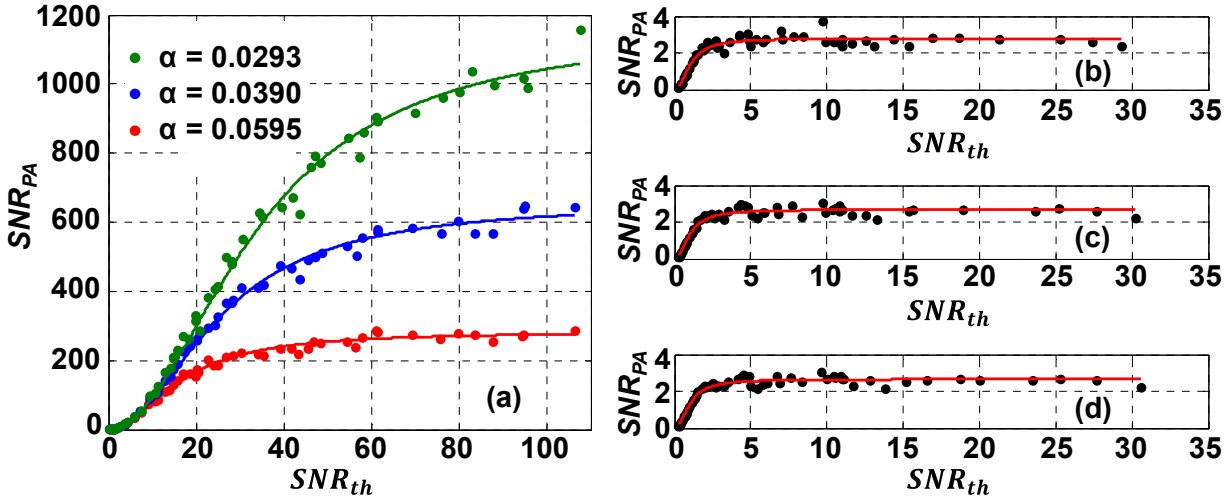

Fig. 3 Measurement results rely on different fluctuation contributors. (a) If the particle number is large, measurement result equals to $1/\alpha^2$. (b)(c)(d) If the particle number is small, the result is only determined by the particle number. (b) α=0.0066. (c) α=0.0284. (d) α=0.0587. For (b), (c), and (d), the black dots are the measurement data and the red curves are the fitting results based on the model.

Next, we applied our method to quantitatively measure five different particle concentration samples. Fig. 4(a) shows measured results with five different preset particle counts of 440, 220, 110, 55, and 27 in the detection volume. The experimental results agree well with the preset values. In addition, we observed that the measured particle count does not change with the laser fluence any longer when the SNR_{th} is high enough. The fitted coefficient $E(N_p)$ in the model was used to quantify the absolute particle count for each sample. As shown in Fig. 4(b), the experimental results agree well with the preset particle counts in the detection volume.

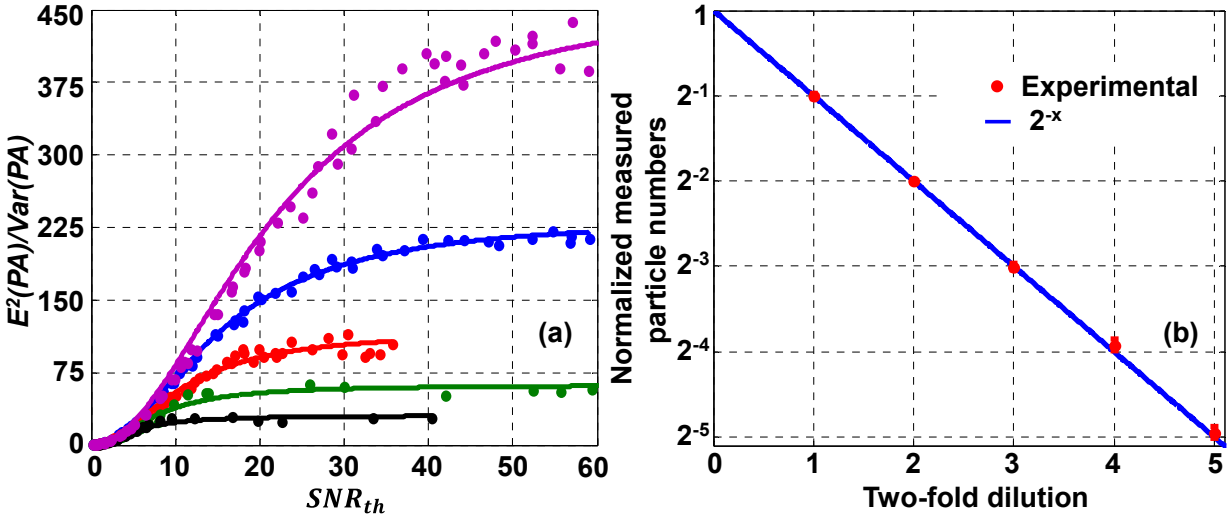

Fig. 4 Measured particle numbers of the same light fluctuation. (a) The relative particle numbers are 1, 1/2, 1/4, 1/8, and 1/16, respectively. (b) Red dot, measured particle numbers. The blue line shows the theoretical relative particle numbers.

4. Discussion

Both the theoretical model and experimental study showed that our method is applicable when the particle count in the detection volume is sufficiently small such that the particle Brownian motion dominates the PA signal fluctuation. If we can control the photon count fluctuation coefficient within 1%, the maximum count of particles that we can measure is on the order of 1000 ($\ll 1/\alpha^2$). By contrast, the minimum measurable count of particles is limited by SNR_{th}. If the count of particles in the detection volume is too small, noise reduces the measuring accuracy significantly. Either particles with larger absorption cross-sections or greater detection volumes can reduce the minimum. Based on our experimental results (Fig. 3(b)-(d)), we conclude that our method can measure as few as three RBCs in the detection volume.

Moreover, as shown in the *Results* section (Fig. 4), our measured particle counts are slightly larger than the preset absolute counts estimated based on the detection volume of 500 μm^3. This is most likely due to the inaccurate estimation of the detection volume. We calculated the detection volume based on the 1/e detection sensitivity field. However, particles not in this volume can still generate PA signals, which will contribute to the total PA signals. If we take those particles into account, the actual detection volume becomes greater.

Finally, as shown in Figs. 3(a), 4(a), and 5(a), when SNR_{th} becomes high enough, the measured particle counts are independent of the SNR_{th} and laser fluence. Although we examined the complete trend in this study with varying SNR_{th}, a measurement with a single, high enough SNR_{th} is sufficient to measure the fluence-independent particle counts in the detection volume.

5. Conclusion

To the best of our knowledge, this is the first study using PAM for fluence-independent particle count measurement by statistically analyzing PA signals. This method has been experimentally verified by using different kinds of samples, including RBCs. Therefore, our method shows promise to quantitatively measure biological samples *in vivo*.

References

[1]. Y. Zhou, C. Zhang, D. K. Yao and L. H. V. Wang, "Photoacoustic microscopy of bilirubin in tissue phantoms," *J Biomed Opt* 17(12), (2012)

[2]. L. H. V. Wang and S. Hu, "Photoacoustic Tomography: In Vivo Imaging from Organelles to Organs," *Science* 335(6075), 1458-1462 (2012)

[3]. J. Y. Liang, Y. Zhou, A. W. Winkler, L. D. Wang, K. I. Maslov, C. Y. Li and L. H. V. Wang, "Random-access optical-resolution photoacoustic microscopy using a digital micromirror device," *Opt Lett* 38(15), 2683-2686 (2013)

[4]. Y. Zhou, J. J. Yao and L. H. V. Wang, "Optical clearing-aided photoacoustic microscopy with enhanced resolution and imaging depth," *Opt Lett* 38(14), 2592-2595 (2013)

[5]. C. Zhang, Y. Zhou, C. Y. Li and L. H. V. Wang, "Slow-sound photoacoustic microscopy," *Appl Phys Lett* 102(16), (2013)

[6]. Y. Zhou, J. Y. Liang, K. I. Maslov and L. H. V. Wang, "Calibration-free in vivo transverse blood flowmetry based on cross correlation of slow time profiles from photoacoustic microscopy," *Opt Lett* 38(19), 3882-3885 (2013)

[7]. J. Y. Liang, Y. Zhou, K. I. Maslov and L. H. V. Wang, "Cross-correlation-based transverse flow measurements using optical resolution photoacoustic microscopy with a digital micromirror device," *J Biomed Opt* 18(9), (2013)

[8]. J. J. Yao, J. Xia, K. I. Maslov, M. Nasiriavanaki, V. Tsytsarev, A. V. Demchenko and L. V. Wang, "Noninvasive photoacoustic computed tomography of mouse brain metabolism in vivo," *Neuroimage* 64(257-266 (2013)

[9]. J. J. Yao, H. X. Ke, S. Tai, Y. Zhou and L. H. V. Wang, "Absolute photoacoustic thermometry in deep tissue," *Opt Lett* 38(24), 5228-5231 (2013)